

Elasticity in Physically Cross-Linked Amyloid Fibril Networks

Yiping Cao,¹ Sreenath Bolisetty,¹ Jozef Adamcik,¹ and Raffaele Mezzenga^{1,2,*}

¹*Department of Health Sciences and Technology, ETH Zurich, Schmelzbergstrasse 9, Zurich 8092, Switzerland*

²*Department of Materials, ETH Zurich, Wolfgang-Pauli-Strasse 10, Zurich 8093, Switzerland*



(Received 5 October 2017; revised manuscript received 2 February 2018; published 13 April 2018)

We provide a constitutive model of semiflexible and rigid amyloid fibril networks by combining the affine thermal model of network elasticity with the Derjaguin-Landau-Verwey-Overbeek (DLVO) theory of electrostatically charged colloids. When compared to rheological experiments on β -lactoglobulin and lysozyme amyloid networks, this approach provides the correct scaling of elasticity versus both concentration ($G \sim c^{2.2}$ and $G \sim c^{2.5}$ for semiflexible and rigid fibrils, respectively) and ionic strength ($G \sim I^{4.4}$ and $G \sim I^{3.8}$ for β -lactoglobulin and lysozyme, independent from fibril flexibility). The pivotal role played by the screening salt is to reduce the electrostatic barrier among amyloid fibrils, converting labile physical entanglements into long-lived cross-links. This gives a power-law behavior of G with I having exponents significantly larger than in other semiflexible polymer networks (e.g., actin) and carrying DLVO traits specific to the individual amyloid fibrils.

DOI: 10.1103/PhysRevLett.120.158103

Amyloid fibrils are β -sheet rich supramolecular polymers resulting from the self-assembly of proteins or peptides [1,2]. *In vivo* they rarely exist as isolated single filaments, but they rather further entangle into percolating networks first and amyloid plaques and deposits afterwards, all with multiple characteristic length scales [1,3]. These structures initially identified in nature, in the context of pathological protein-prone neurodegenerative diseases, have also been discovered as key functional components in biological organisms ranging from bacteria to humans [1,4,5]. Artificial variants of these systems are now also emerging as functional materials for the design of ultralight aerogels, drug delivery platforms, cell scaffolds, artificial bones, degradable films, solar energy conversion, and water purification [6,7]. Many of these applications depend strongly on the structural and mechanical properties of the amyloid fibril networks [7,8]. Yet, compared to other biological networks, such as elastin for example, the structure-properties relationship in amyloid networks, and how physical properties of the individual fibrils are reflected at larger scales, is significantly less established. A theoretical framework to describe the elasticity of semiflexible or rigid networks has been developed over the last two decades, primarily to study actin gels [9–15]. These approaches have been particularly successful to describe the dependency of elasticity on polymer concentration, chain flexibility [15,16], cross-linking procedure [12–14], and cross-linking density [15]. Other factors, such as the connectivity architectures [11], the affinity and size of cross-linker [10], and the deformation nature (affine or nonaffine) [9], have also been studied. The predicted elasticity dependencies above have been validated primarily against actin [9–15], collagen [17], fibrin [18], and intermediate filaments networks

[19,20], all systems with moderate surface charge density and exhibiting a relatively low rheological dependence on ionic strength [12,19–21]. Therefore, it is still unclear whether the same description can be adopted to study other biological networks of stiff and semiflexible polymers, such as amyloid fibrils, where the nature of physical interactions among individual filaments can be significantly different as a result of the complex interplay between Derjaguin-Landau-Verwey-Overbeek (DLVO) [22,23], hydrophobic, and hydrogen bonding interactions. Indeed, although previous works demonstrated the formation of hydrogels from mature amyloid fibrils by the addition of sodium chloride [24], alteration of pH and addition of calcium [25], or thiolation [26], the quantitative analysis on the network elasticity is still not clearly described, nor it is understood how the elasticity of amyloid fibril networks is ruled by intrinsic and extrinsic factors, such as chain flexibility, contour length, ionic strength, etc. A proper physical understanding of the basis of amyloid networks elasticity would not only shed light on the fundamentals, but also foster the expanding field of applications of amyloid fibrils in nanotechnology. Here, we investigate the elasticity of amyloid fibril networks from β -lactoglobulin and lysozyme at different fibril concentrations, chain flexibilities, and contour lengths. We use ionic strength to modulate the strength of filament-filament interactions and we show that the theoretical background of the elasticity of semiflexible or rigid networks, when duly combined with the DLVO theory to quantify the interaction strength, provides a robust framework to describe the elasticity of amyloid hydrogels in a very broad window of experimental conditions.

We use β -lactoglobulin fibrils as the first model amyloid network because these fibrils have been both deeply

characterized at the single fibrils level [27] and used in a number of highly promising applications already [28–30]. Individual β -lactoglobulin amyloid fibrils possess semiflexible multistranded twisted ribbonlike structures, with an average diameter ~ 4 nm, a contour length L spanning several micrometers, and a persistence length $l_p \sim 2$ μ m [27]. Furthermore, these fibrils can be, under specific conditions, structurally modified into fully rigid fibrils [31]. The nature of the network is complex: Loveday *et al.* demonstrated that β -lactoglobulin or whey protein isolate monomer could form fibrillar hydrogels in the presence of salt by heating at low pHs, as a result of simultaneous fibrillization and cross-linking of protein monomers [32].

β -lactoglobulin was purified according to previous protocols [33], and then a 2 wt% protein solution was heated at pH 2 and 90 °C for 5 h under stirring to produce mature semiflexible amyloid fibrils; these same fibrils were further homogenized in order to prepare rigid fibrils [31]. The structural information of individual fibrils was examined by atomic force microscopy (AFM) and analyzed by our open source software FiberApp [34]. Elastic modulus G' and loss modulus G'' of fibril hydrogels were monitored by a stress-controlled rheometer with a cone-plate geometry. An applied strain of 1.0% was used to ensure that all measurements were in the linear elastic regime. Different fibril concentrations were obtained either by diluting a 2 wt% fibril solution with pH 2 Milli-Q water or by concentrating the same solution by airflow. Ionic strength was adjusted by the addition of sodium chloride, potassium chloride and calcium chloride.

AFM imaging of mature β -lactoglobulin amyloid fibrils [Fig. 1(a)] shows multistranded fibrils with an average

contour length $\langle L \rangle = 2137$ nm and persistence length $l_p = 2438$ nm (see Supplemental Material [35]). Figure 1(b) shows an AFM image of shortened fibrils with $\langle L \rangle = 366$ nm [35]. The fibril flexibility can be quantified by comparison of L and l_p . A fibril is considered to be flexible when $l_p \ll L$, rigid when $l_p \gg L$, and semiflexible when $l_p \approx L$ [34]. Therefore, the mature and short fibrils can be classified as semiflexible and (approximately) rigid fibrils, respectively.

The gelation condition of both fibrils was identified by altering the fibril concentration c and ionic strength I , as shown in the phase diagrams [35]. Transparent (at low ionic strengths, ca. $I < 50$ mM NaCl) and translucent (at high ionic strengths, ca. $I > 135$ mM NaCl) solutions are observed for both fibrils, which is consistent with the phase diagram of semiflexible fibrils in the previous study [24]. The elasticities of both fibril gels were investigated by rheological measurements in the ionic strength range of 50–110 mM NaCl. Figure 1(c) shows the frequency sweep of a representative semiflexible fibril hydrogel. Clearly, G' exceeds G'' and is nearly frequency independent, suggesting the amyloid fibril network is typically elastic. In comparison, the rigid fibrils showed a relatively weaker elastic behavior at identical c and I [Fig. 1(d)]. This can be explained by the lower number of cross-linking points at the same total fibril contour length for shorter fibrils. The network elasticity, plateau modulus G_0 , was characterized by studying the value of G' at frequency 1 rad/s. The graphical representation outlined by summarizing G_0 at different I and c shows that the elasticity of amyloid fibril networks can be tuned over 2 orders of magnitude, at least [35].

To systematically study the origin of the elasticity, for both semiflexible and rigid fibrils, we plot the G_0 dependency on I at fixed c and the other way around. Amyloid fibril hydrogels show increasing G_0 with raising I . From previous studies, it is known that the addition of sodium chloride in mature fibrils does not alter their morphology [37], inferring that the increase in G_0 arises from the alteration of the network structures instead of the properties of individual fibrils. Quantitative analysis shows an average power law $G_0 \sim I^{4.4 \pm 0.2}$ [Fig. 2(a)], i.e., a characteristic exponent much higher than those of other filament networks cross-linked by the divalent ions or specifically binding proteins, such as vimentin filament in calcium or magnesium (with an exponent of 0.51) [19], neurofilament in magnesium (with an exponent of 0.60) [20], and actin filament in scruin or fascin (with an exponent of 1.5–2.0) [12,21]. This unexpected finding implies a different mechanism for the percolating amyloid fibril network on addition of sodium chloride, as discussed further below. Figure 2(b) further examines the G_0 dependency on c at fixed I , and an average scaling law $G_0 \sim c^{2.2 \pm 0.1}$ is found, i.e., in good agreement with the theory of cross-linked networks predicting 2.2 for semiflexible polymers [12,13,15] and with other experimental studies such as the cross-linked actin or

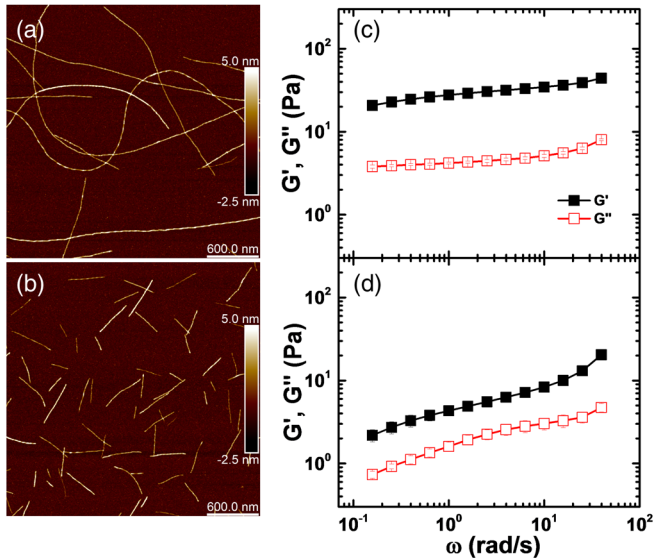


FIG. 1. AFM images and frequency sweeps of β -lactoglobulin amyloid fibrils. AFM images of (a) semiflexible and (b) rigid fibrils. Elastic modulus G' and loss modulus G'' of (c) semiflexible and (d) rigid fibrils at fibril concentration $c = 2$ wt% and ionic strength $I = 110$ mM NaCl.

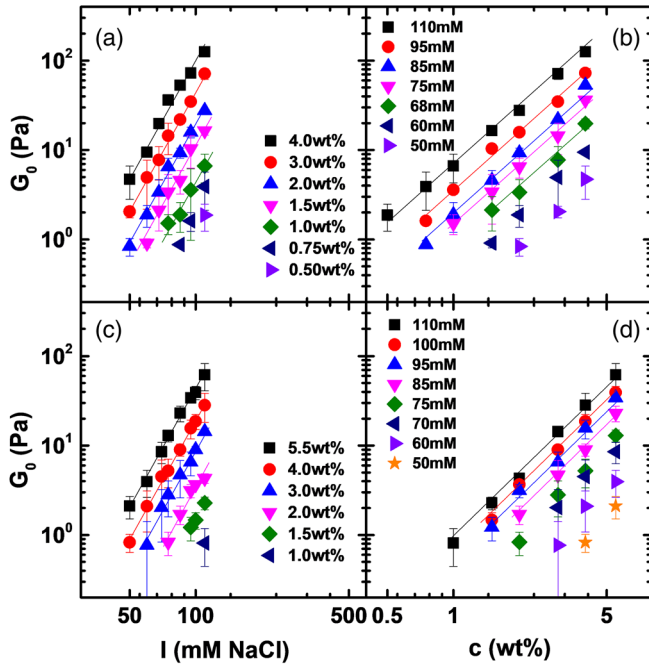


FIG. 2. Elastic modulus G_0 of β -lactoglobulin fibril networks at different ionic strength I and fibril concentration c . Semiflexible fibrils: (a) G_0 versus I at fixed c ; the solid lines indicate a scaling of $G_0 \sim I^{4.4}$; (b) G_0 versus c at fixed I ; the solid lines indicate a scaling of $G_0 \sim c^{2.2}$. Rigid fibrils: (c) G_0 versus I at fixed c ; the solid lines indicate a scaling of $G_0 \sim I^{4.4}$; (d) G_0 versus c at fixed I ; the solid lines indicate a scaling of $G_0 \sim c^{2.4}$.

intermediate filament (exponent 2.0–2.5) [19–21], collagen (exponent 2.2–2.4) [17], fibrin (exponent 2.2) [18], stiff DNA (exponent 2.3) [38], and synthetic peptide filament networks (exponent 2.2–2.7) [39].

For rigid fibrils, scaling behaviors $G_0 \sim I^{4.4 \pm 0.2}$ and $G_0 \sim c^{2.4 \pm 0.1}$ are found, as displayed in Figs. 2(c) and 2(d). In this case, G_0 exhibits a slightly stronger dependency on c compared to semiflexible ones and above the exponent of infinitely stiff or pure rod, predicted to be two [16]. Yet, the exponent still falls into the range of the scaling exponents for the cross-linked network, as mentioned above. In contrast, the G_0 dependencies on I are identical for both fibrils, indicating that the mechanism for cross-linking the amyloid fibril networks followed by the monovalent salt does not depend of fibril length and flexibility. Furthermore, replacing NaCl with other monovalent (KCl) and divalent (CaCl_2) ions, does not produce significant changes in either the power law or the experimental exponent [35], pointing at pure electrostatic and not ion-specific effects. Normalizing G_0 by the fibril concentration dependency $c^{2.2}$ for semiflexible fibrils and $c^{2.4}$ for rigid fibrils results in a collapse of all data points on one single master curve $G_0 \sim I^{4.4}$ [Fig. 3(a)]. Normalizing G_0 by the ionic strength dependency $I^{4.4}$ produces the master curves, respectively, for semiflexible $G_0 \sim c^{2.2}$ and rigid $G_0 \sim c^{2.4}$ fibrils [Fig. 3(b)]. The good overlaps further validate the scaling dependencies of G_0 on I and c .

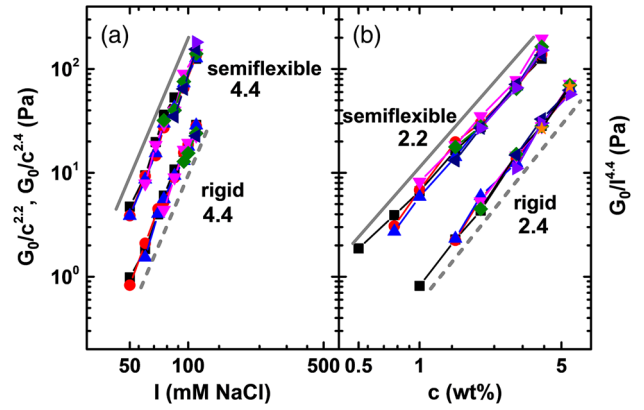


FIG. 3. Normalized G_0 of β -lactoglobulin fibril networks. (a) G_0 are normalized by $G_0 \sim c^{2.2}$ (semiflexible fibrils) or $G_0 \sim c^{2.4}$ (rigid fibrils) with reference to G_0 at $c = 4$ wt% showing an identical scaling law $G_0 \sim I^{4.4}$ for both fibrils; the symbols for different fibril concentrations are identical to those in Figs. 2(a) and 2(c). (b) G_0 are normalized by $G_0 \sim I^{4.4}$ with reference to G_0 at $I = 110$ mM. The scaling exponents of 2.2 and 2.4 are, respectively, for semiflexible and rigid fibrils; the symbols for different ionic strengths are identical to those in Figs. 2(b) and 2(d).

For gelled amyloid fibril systems, G' is larger than G'' , exhibiting no crossover in the investigated frequency range (0.1–100 rad/s). This kind of rheological behavior suggests the fibril networks have a large characteristic relaxation time, implying the cross-linking parts of the networks are long-lived junctions and not simple entanglements [40]. Moreover, G_0 for entangled networks has a much weaker dependency on c , as verified by both rheological measurements and theoretical considerations: an exponent of 1.4 was first found by Isambert and Maggs [41]. In contrast, the dependencies of G_0 on c for the amyloid fibril networks here are very similar to those predicted for the cross-linked networks [12,13,15]. It is important to note, however, that the fibril hydrogels in the present investigation are purely physical networks; no chemical cross-linking strategy is involved or has been added during the formation of amyloid fibril networks. Based on the unexpectedly high scaling exponent of G_0 on c and I , it becomes plausible to expect that the amyloid fibril hydrogels become, at least in the accessible frequency domain, lastingly cross-linked upon salt addition. In other words, ions mediate attractive interactions between the positively charged fibrils, which once in contact with each other, become cross-linked analogous to chemically cross-linked networks. With this in mind, the affine thermal model developed by MacKintosh *et al.* [15] and Weitz and co-workers [12,13] can be applied, with some needed modifications, also to the present amyloid network in the presence of salts. In the affine thermal model, the elasticity can be expressed as [12,13,15]

$$G_0 \sim \frac{\kappa_0^2}{k_B T \xi^2 l_c^3}, \quad (1)$$

where κ_0 is the bending modulus, k_B is the Boltzmann constant, T is the absolute temperature, l_c is the cross-link length, and ξ is the network mesh size; $\xi \sim c^{-1/2}$ for $l_p \gg \xi$ [42]. For classical polyelectrolytes, κ_0 (or l_p) could be certainly influenced by I , as the ionic screening effect is weakening the intramolecular electrostatic repulsion [43]. However, for amyloid fibrils, the ionic screening effect on l_p is negligible [44], as l_p arises by the hydrogen bonding β sheets and is orders of magnitude above the Debye length. Therefore, the tunability of G_0 by varying I and c is only associated with changes in l_c and ξ .

As pointed out by Odijk [45], the most likely binding sites on polymers for effective cross-linking are sites where polymer strands interact sterically, i.e., the entanglement parts. Therefore it is reasonably postulated that

$$l_c \sim l_e I^x, \quad (2)$$

where l_e is the entanglement length, and x is a dimensionless scaling parameter capturing the cross-linking induced by I . For semiflexible fibrils, $l_e \sim (\kappa_0/k_B T)^{1/5} c^{-2/5}$ [15]. By using Eq. (1), the predicted elasticity modulus of semiflexible fibrils can be written as

$$G_0 \sim c^{11/5} I^{-3x}. \quad (3)$$

In contrast, $l_e \approx \xi \sim c^{-1/2}$ for rigid fibrils, in this case, G_0 scales as

$$G_0 \sim c^{5/2} I^{-3x}. \quad (4)$$

These theoretically predicted dependencies of G_0 on c of $11/5 = 2.2$ and $5/2 = 2.5$ for semiflexible and rigid fibrils, respectively, are fully consistent with the experimental results shown in Fig. 3 featuring corresponding exponents of 2.2 ± 0.1 and 2.4 ± 0.1 . The 0.1 difference between theoretical and experimental exponents for short fibrils may arise from their imperfect rigid nature. Thus, the stronger G_0 dependence on c for rigid fibrils arises from the steeper dependence of entanglement density on mass concentration.

As previously noted, G_0 has the same dependence on I for both fibrils and much higher exponent was observed compared to other cross-linked filament networks. This unexpected behavior can be elucidated by the DLVO theory. As postulated above, the cross-links caused by I occur at the entanglement contacts. To model the physical interactions at entanglement points, we assume the fibrils as a sequence of spheres inscribed within the fibril cylinders and account the total potential between nearest constitutive spheres only, as this is expected to produce the right scaling form with the ionic strength. The interaction potential F_{DLVO} between such two constitutive charged particles R , whose surface is separated by a distance D , can then be written as the sum of the screened electrostatic repulsion in

the Debye-Hückel approximation and the van der Waals attractive contribution [22,23,46]

$$F_{DLVO} \approx \frac{2\pi\sigma^2 R}{\kappa^2 \epsilon_0 \epsilon_r} e^{-\kappa D} - \frac{AR}{12D} \quad (5)$$

where σ is the surface charge density of the particles, ϵ_0 is the dielectric permittivity in a vacuum (8.85×10^{-12} F m $^{-1}$), ϵ_r is the relative dielectric permittivity in water (80.1), A is the Hamaker constant, and κ^{-1} is the Debye length, expressed as $\kappa^{-1} = \sqrt{\epsilon_0 \epsilon_r k_B T / 2N_A e^2 I}$; here $k_B = 1.38 \times 10^{-23}$ JK $^{-1}$, $T = 296$ K, N_A is the Avogadro constant (6.02×10^{23} mol $^{-1}$), e is the elementary charge (1.6×10^{-19} C), and I is the total ionic strength (in mol m $^{-3}$). For β -lactoglobulin fibrils, $\sigma \approx 0.03$ C m $^{-2}$ [35] and $R = 2$ nm [27]; A can be assumed to be on the order of $\approx 3k_B T$, which is a typical approximate value of the Hamaker constant of proteins in water [46]. Using the above-mentioned values with Eq. (5) yields

$$\frac{F_{DLVO}}{k_B T} \approx 2 \left(\frac{183.4}{I} e^{-0.104\sqrt{I}D} - \frac{1}{4D} \right), \quad (6)$$

where D is now expressed in nanometers. In order for a long-lived cross-link to occur, contact needs to be established among two fibrils; i.e., the associated DLVO energy barrier needs to be overcome, with an aggregation probability $p = e^{-F/k_B T}$, where F is the maximum of $F_{DLVO} - D$ curve [Fig. 4(a)]. This leads to a functional dependence of p versus I which, in the limited range of I considered, can be

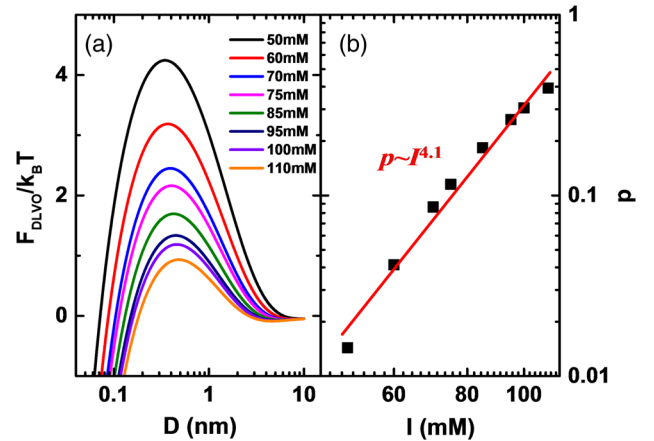


FIG. 4. The probability of cross-linking at the entanglement rationalized by DLVO theory. (a) Interaction potential $F_{DLVO}/k_B T$ versus distance D of nearest constitutive spheres at different ionic strengths. (b) The probability of cross-linking at the entanglement p as a function of ionic strength I ; in the investigated ionic strength range, the functional form can be approximated to a scaling law of the type $p \sim I^{4.1}$, as shown by the red solid line.

approximated to a simple power law of the type $p \sim I^{4.1}$ [Fig. 4(b)].

In a three-dimensional network, the overall volume of the network can be written as $V_{\text{total}} = l_c^3 N_c = l_e^3 N_e$ [35], where N_c and N_e are the total number of cross-link and entanglement points, respectively. But the probability p of a cross-link occurring from an entanglement is simply N_c/N_e , and thus

$$l_c \approx l_e p^{-1/3}. \quad (7)$$

This then provides the correct form for the scaling exponent in Eq. (2), and yields via Eqs. (3) and (4), $G_0 \sim p \sim I^{4.1}$ for both fibril gels, which is well in line with the rheological measurements (experimental scaling 4.4). This indicates the cross-linking mechanisms occurring in amyloid fibril networks: once the electrostatic barrier is overcome and fibrils come in contact, the adhesive forces among them become sufficiently strong to make their contact assimilable to a cross-link, at least in the timescales experimentally accessible. This is very much consistent with the acclaimed irreversible aggregation among proteinaceous colloids.

It is important to point out that the present approach is not specific to the β -lactoglobulin amyloids, but is generally applicable to other amyloid networks as well. For example, by following an analog series of experiments and analysis in lysozyme amyloid gels, identical scaling exponents of 2.2 ± 0.1 and 2.4 ± 0.1 are found for the scaling of G_0 with c in semiflexible and rigid networks, respectively [35]. For the ionic strength dependence, G_0 is found to scale in this case as $I^{3.8 \pm 0.2}$ experimentally, again in good agreement with the $I^{4.0}$ theoretical prediction for lysozyme fibrils [35]. This indicates that the combined DLVO and affine network theories offer a general framework to study amyloid fibril networks, where the scaling exponents of the stiffness versus density are universal, while those related to electrostatic barriers carry DLVO traits specific to the individual system considered [35].

In summary, by combining the affine thermal model of the elasticity of rigid and semiflexible polymers with the DLVO theory, we have been able to capture the correct scaling behavior of the elasticity with concentration and ionic strength for both semiflexible and rigid amyloid networks. A key point is the possibility of letting physical entanglements evolve into long-lived cross-links once the electrostatic barrier energy is overcome in presence of salt. These results expand and complete our understanding on the elasticity of nonentropic networks, in particular, when nonspecifically binding ions modulate the final stiffness.

The authors thank Professor Peter Fischer at the Laboratory of Food Process Engineering (ETH Zurich) for granting access to rheological measurements and thank Lukas Böni for technical training. Valuable discussions

with Dr. Salvatore Assenza and Dr. Jianguo Zhao are greatly acknowledged. Y.C. thanks the China Scholarship Council for financial support.

*raffaele.mezzenga@hest.ethz.ch

- [1] T. P. J. Knowles and M. J. Buehler, *Nat. Nanotechnol.* **6**, 469 (2011).
- [2] R. Riek and D. S. Eisenberg, *Nature (London)* **539**, 227 (2016).
- [3] R. Papparcone, S. W. Cranford, and M. J. Buehler, *Nanoscale* **3**, 1748 (2011).
- [4] J. W. Kelly, *Nat. Struct. Biol.* **9**, 323 (2002).
- [5] D. M. Fowler, A. V. Koulov, C. Alory-Jost, M. S. Marks, W. E. Balch, and J. W. Kelly, *PLoS Biol.* **4**, e6 (2006).
- [6] G. Wei, Z. Su, N. P. Reynolds, P. Arosio, I. W. Hamley, E. Gazit, and R. Mezzenga, *Chem. Soc. Rev.* **46**, 4661 (2017).
- [7] T. P. J. Knowles and R. Mezzenga, *Adv. Mater.* **28**, 6546 (2016).
- [8] U. Shimanovich, I. Efimov, T. O. Mason, P. Flagmeier, A. K. Buell, A. Gedanken, S. Linse, K. S. Åkerfeldt, C. M. Dobson, D. A. Weitz, and T. P. J. Knowles, *ACS Nano* **9**, 43 (2015).
- [9] C. P. Broedersz and F. C. MacKintosh, *Rev. Mod. Phys.* **86**, 995 (2014).
- [10] O. Lieleg, M. M. A. E. Claessens, and A. R. Bausch, *Soft Matter* **6**, 218 (2010).
- [11] E. M. Huisman, T. van Dillen, P. R. Onck, and E. van der Giessen, *Phys. Rev. Lett.* **99**, 208103 (2007).
- [12] J. H. Shin, M. L. Gardel, L. Mahadevan, P. Matsudaira, and D. A. Weitz, *Proc. Natl. Acad. Sci. U.S.A.* **101**, 9636 (2004).
- [13] M. L. Gardel, J. H. Shin, F. C. MacKintosh, L. Mahadevan, P. Matsudaira, and D. A. Weitz, *Science* **304**, 1301 (2004).
- [14] B. Hinner, M. Tempel, E. Sackmann, K. Kroy, and E. Frey, *Phys. Rev. Lett.* **81**, 2614 (1998).
- [15] F. C. MacKintosh, J. Käs, and P. A. Janmey, *Phys. Rev. Lett.* **75**, 4425 (1995).
- [16] J. L. Jones and C. M. Marques, *J. Phys. II (France)* **51**, 1113 (1990).
- [17] A. J. Licup, S. Münster, A. Sharma, M. Sheinman, L. M. Jawerth, B. Fabry, D. A. Weitz, and F. C. MacKintosh, *Proc. Natl. Acad. Sci. U.S.A.* **112**, 9573 (2015).
- [18] I. K. Piechocka, K. A. Jansen, C. P. Broedersz, N. A. Kurniawan, F. C. MacKintosh, and G. H. Koenderink, *Soft Matter* **12**, 2145 (2016).
- [19] Y. C. Lin, C. P. Broedersz, A. C. Rowat, T. Wedig, H. Herrmann, F. C. MacKintosh, and D. A. Weitz, *J. Mol. Biol.* **399**, 637 (2010).
- [20] Y. C. Lin, N. Y. Yao, C. P. Broedersz, H. Herrmann, F. C. MacKintosh, and D. A. Weitz, *Phys. Rev. Lett.* **104**, 058101 (2010).
- [21] O. Lieleg, M. M. A. E. Claessens, C. Heussinger, E. Frey, and A. R. Bausch, *Phys. Rev. Lett.* **99**, 088102 (2007).
- [22] B. Derjaguin and L. Landau, *Prog. Surf. Sci.* **43**, 30 (1993).
- [23] E. J. W. Verwey and J. T. G. Overbeek, *Theory of the Stability of Lyophobic Colloids* (Elsevier, New York, 1948).
- [24] S. Bolisetty, L. Harnau, J. M. Jung, and R. Mezzenga, *Biomacromolecules* **13**, 3241 (2012).

- [25] C. Veerman, H. Baptist, L. M. C. Sagis, and E. van der Linden, *J. Agric. Food Chem.* **51**, 3880 (2003).
- [26] C. D. Munialo, H. H. J. de Jongh, K. Broersen, E. van der Linden, and A. H. Martin, *J. Agric. Food Chem.* **61**, 11628 (2013).
- [27] J. Adamcik, J. M. Jung, J. Flakowski, P. De Los Rios, G. Dietler, and R. Mezzenga, *Nat. Nanotechnol.* **5**, 423 (2010).
- [28] C. Li, J. Adamcik, and R. Mezzenga, *Nat. Nanotechnol.* **7**, 421 (2012).
- [29] Y. Shen, L. Posavec, S. Bolisetty, F. M. Hilty, G. Nyström, J. Kohlbrecher, M. Hilbe, A. Rossi, J. Baumgartner, M. B. Zimmermann, and R. Mezzenga, *Nat. Nanotechnol.* **12**, 642 (2017).
- [30] S. Bolisetty and R. Mezzenga, *Nat. Nanotechnol.* **11**, 365 (2016).
- [31] J. Zhao, S. Bolisetty, J. Adamcik, J. Han, M. P. Fernández-Ronco, and R. Mezzenga, *Langmuir* **32**, 2492 (2016).
- [32] S. M. Loveday, S. G. Anema, and H. Singh, *Int. Dairy J.* **67**, 35 (2017).
- [33] D. Vigolo, J. Zhao, S. Handschin, X. Cao, A. J. Demello, and R. Mezzenga, *Sci. Rep.* **7**, 1211 (2017).
- [34] I. Usov and R. Mezzenga, *Macromolecules* **48**, 1269 (2015).
- [35] See Supplemental Material at <http://link.aps.org/supplemental/10.1103/PhysRevLett.120.158103> for the structural information of fibrils, phase and elasticity diagrams, surface charge density, three-dimensional network illustration, scaling behaviors in lysozyme fibrils, and exponent difference analysis, which includes Refs. [27,34,36].
- [36] K. Makino and H. Ohshima, *Langmuir* **26**, 18016 (2010).
- [37] J. Adamcik and R. Mezzenga, *Soft Matter* **7**, 5437 (2011).
- [38] T. G. Mason, A. Dhople, and D. Wirtz, *Macromolecules* **31**, 3600 (1998).
- [39] P. H. J. Kouwer, M. Koepf, V. A. A. Le Sage, M. Jaspers, A. M. van Buul, Z. H. Eksteen-Akeroyd, T. Woltinge, E. Schwartz, H. J. Kitto, R. Hoogenboom, S. J. Picken, R. J. M. Nolte, E. Mendes, and A. E. Rowan, *Nature (London)* **493**, 651 (2013).
- [40] B. Ozbas, K. Rajagopal, J. P. Schneider, and D. J. Pochan, *Phys. Rev. Lett.* **93**, 268106 (2004).
- [41] H. Isambert and A. C. Maggs, *Macromolecules* **29**, 1036 (1996).
- [42] P. G. D. Gennes, *Scaling Concepts in Polymer Physics* (Cornell University Press, Ithaca, 1979).
- [43] J. P. Berezney and O. A. Saleh, *Macromolecules* **50**, 1085 (2017).
- [44] P. Aymard, T. Nicolai, D. Durand, and A. Clark, *Macromolecules* **32**, 2542 (1999).
- [45] T. Odijk, *Macromolecules* **16**, 1340 (1983).
- [46] R. Mezzenga and P. Fischer, *Rep. Prog. Phys.* **76**, 046601 (2013).